a Wall for Large Schmidt Numbers," *AIChE J.*, 23, 28 (1977).
Sirkar, K. K., "Turbulence in the Immediate Vicinity of a Wall and Fully Developed Mass Transfer at High Schmidt Numbers," Ph.D. thesis, Univ. Ill., Urbana (1969).
———, and T. J. Hanratty, "Relation of Turbulent Mass Transfer to a Wall at High Schmidt Numbers to the Velocity Field," *J. Fluid Mech.*, 44, 589 (1970).
Van Shaw, P., "A Study of the Fluctuation and the Time Average of the Rate of Mass Transfer to a Pipe Wall," Ph.D. thesis, Univ. Ill., Urbana (1963).
———, and T. J. Hanratty, "Fluctuations in the Local Rate of Turbulent Mass Transfer to a Pipe Wall," *AIChE J.*, 10, 475 (1964).

Manuscript received July 22, 1976; revision received November 17, and accepted November 19, 1976.

A Compartmental Dispersion Model for the Analysis of Mixing in Tube Networks

JAMES S. ULTMAN

Department of Chemical Engineering and The Bioengineering Program The Pennsylvania State University University Park, PA 16802

and

HAL S. BLATMAN

The Medical College of Pennsylvania Philadelphia, PA 19129

A compartmental dispersion model of longitudinal mixing in tube networks has been developed. The ability of this model to predict the impulse response of helium, benzene vapor, and sulfur hexafluoride tracer gases in two and in five generation symmetric network models of the large airway system of the lung has been tested over an air flow range of 1 to 400 ml/s.

The results imply that velocity profile distortion and secondary flows in branching regions have only a small effect upon the overall longitudinal mixing when flow is directed toward the higher-order generations. On the other hand, accurate prediction of the data requires adequate treatment of the finite rate of evolution of the Taylor dispersion occurring in these tube networks.

SCOPE

The tracer dispersion technique applied to both the cardiovascular and pulmonary systems has become an accepted, if not routine, method of diagnosis and function testing. In the lungs especially, where there are several reliable models of the flow network geometry (see, for example, Weibel, 1963; Horsfield and Cumming, 1968*a*), it should be possible to predict the tracer dispersion from first principles. Or, what is the more relevant biomedical problem, given a set of tracer dispersion data, it might be possible to recognize the nature of deviations in the system geometry from an established norm.

The objective of this study was to develop an approximate method of predicting tracer dispersion for laminar flow through a tube network of known geometry. Though attention was focused upon symmetrically branched models of the pulmonary airway system, the methods can be extended to other tube networks as well.

Although a wealth of pulmonary dispersion data obtained from human subjects exists, its interpretation has led to inconsistent conclusions among the various investigators. For example, following a 60 ml inspiration of a helium-oxygen mixture, Briscoe et al. (1954) found detectable levels of helium in the gas sampled between 750 and 1 250 ml expired. These investigators concluded that the convective displacement of the helium in a parabolic front must be responsible for its unexpectedly high penetration. Power (1969) repeated the same experiment using a mixture of hydrogen and sulfur hexafluoride in air and concluded that molecular diffusion was of primary importance since the helium consistently penetrated deeper than the sulfur hexafluoride.

The principal source of confusion in these studies stems from an oversimplified analysis of the data. In particular, we feel that in analyzing pulmonary airway transport, one must allow for significant contributions from several simultaneous mixing modes. Wilson and Lin (1970) made this point by estimating the relative importance of various tubular mixing mechanisms in Weibel's (1963) symmetric model of lung geometry; in this model, the pulmonary tree is comprised of a set of twenty-three generations of bifurcating tubes originating at the trachea. Wilson and Lin's computations indicate that transport by pure convection is most important in the upper eight pulmonary airway generations, Taylor dispersion becomes significant in the following four generations, while axial diffusion is an important factor in the last eleven generations. Thus, in developing an algorithm for predicting tracer dispersion in the lungs, we have attempted to simultaneously account for gas transport by convection, axial dispersion, and axial diffusion.

Correspondence concerning this paper should be addressed to James S. Ultman.

CONCLUSIONS AND SIGNIFICANCE

In this study, the analysis of Gill and Sankarasubramanian (1970) for axial dispersion in straight tubes has been utilized within the framework of a compartmental representation of tube networks. The degree of tracer dispersion predicted by this analysis was compared to gas phase impulse-response data obtained in two and five generation physical models of the large airways in the human lung.

Our results indicate that the compartmental network dispersion theory does an excellent job of predicting the data. Because the theory does not consider the secondary flows and velocity profile distortion occurring at points of tube branching, we conclude that they only have a second-order effect with respect to longitudinal mass transport processes. Moreover, the theory does account for the finite evolution rate of the axial dispersion. If, instead, the asymptotic dispersion formulation of Taylor (1953) were used, the analysis would grossly overestimate longitudinal mixing in the physical models that were studied.

Although only symmetric tube networks have been studied in this work, the analysis can be extended to more complex networks in order to examine other effects such as geometric asymmetries and nonuniform flow distribution.

The use of inert gas dispersion to evaluate the mixing characteristics of the pulmonary airway system is an accepted experimental tool as well as a routine clinical method of pulmonary function evaluation. Although the tracer gas is, in most cases, introduced at a constant rate into inspired air and sampled continuously during expiration, Cumming et al. (1969) demonstrated the feasibility of observing the response to an inspired impulse of tracer gas. As a result of previous tracer experiments, a wide range of possible mixing mechanisms has been implicated in the lung, including pure convection (Briscoe et al., 1954), axial diffusion (Power, 1969; Cumming et al., 1967), Taylor dispersion (Kvale et al., 1975; Johnson and Van Liew, 1974), radial convective mixing at branch points (Scherer et al., 1975), residence time distribution effects (Yu, 1975; Horsfield and Cumming, 1968*b*), and cardiogenic effects (Engel et al., 1973; Bartels et al., 1954). Yet, the important problem of assessing the relative contribution of each of these mechanisms to the overall degree of dispersion has not been satisfactorily solved.

The two limiting convective diffusion processes, pure convection and axial dispersion, were first elucidated in the work of G. I. Taylor (1953). To what extent these processes can, in conjunction with axial diffusion, account for the impulse response in branched tube networks is the key question which motivated this study. In Taylor's analysis, axial transport of a solute flowing through a straight tube was expressed by the differential equation

$$\frac{\partial C}{\partial t} + u\frac{\partial C}{\partial x} = D\frac{\partial^2 C}{\partial x^2} \tag{1}$$

The effective axial mixing coefficient (D) can be expressed as the sum of a binary molecular diffusivity ($\mathcal{D}$) and a dispersion coefficient (D') which in general may be a function of x, t, u, $\mathcal{D}$, and the tube radius (a):

$$D = \mathcal{D} + D'(x, t; u, \mathcal{D}, a) \tag{2}$$

For fully developed laminar flow in sufficiently long tubes, corresponding to long residence times of solute in the tube, Taylor demonstrated that the dispersion coefficient equals $u^2a^2/48\mathcal{D}$. This formulation of D' is often called the Taylor dispersion coefficient. For very short residence times, Taylor reasoned that D' can be attributed solely to the parabolic displacement of solute caused by the laminar velocity profile. This process is often termed pure convective transport.

Employing Taylor's analysis, Wilson and Lin (1970) estimated where in Weibel's (1963) model 'A' of airway geometry the limiting values of D' are reached. This geometric model is mathematically appealing in that all branch lengths, all branch diameters, and all branch angles within a given generation are equal (Figure 1). These investigators found that pure convection dominated Taylor dispersion in the upper eight airway generations, while the reverse was true for generations nine through twenty-three. Moreover, they concluded that axial molecular diffusion outweighed both pure convection and Taylor dispersion for generations twelve through twenty-three. Thus, Wilson and Lin established that there is a continuous transition from pure convection to Taylor dispersion in the pulmonary airways. Under these conditions, the asymptotic analysis of Taylor alone cannot be quantitatively employed to predict the overall impulse response.

On the other hand, the work of Gill and Sankarasubramanian (1970) provides a continuous form for D' as a function of the time elapsed after an impulse is introduced at $x = 0$.

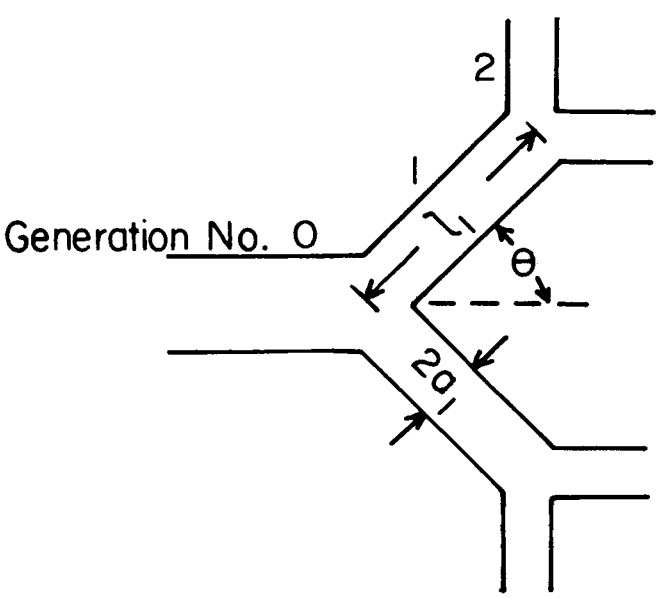

Fig. 1. Schematic representation of a two-generation symmetric tube network.

$$D' = \frac{a^2u^2}{\mathcal{D}}\left(\frac{1}{48} - 16\sum_{n=1}^{\infty} B_n e^{-\lambda_n^2\tau}\right) \quad (3)$$

Here B_n and λ_n are constants defined in terms of Bessel functions of integer order, J_n

$$J_1(\lambda_n) = 0 \quad (4)$$

$$B_n = \frac{J_3(\lambda_n)J_2(\lambda_n)}{\lambda_n^5[J_0(\lambda_n)]^2} \quad (5)$$

and τ is a dimensionless time

$$\tau = t\left(\frac{\mathcal{D}}{a^2}\right) \quad (6)$$

The first term on the right-hand side of Equation (3) is the Taylor dispersion coefficient, while the second term is due to unfulfilled Taylor dispersion. That is, this term accounts for the transition from pure convection at $t = 0$ to Taylor dispersion at $t \to \infty$. It is the existence of this explicit equation for D' that makes a realistic analysis of dispersion in a branched tube network possible.

Specifically, we will demonstrate how the impulse response predicted by Equation (3) for individual tube branches can be incorporated into a compartmental model in order to predict the overall dispersion occurring along a particular transport path of a tube network. This theory will be compared to impulse-response data obtained from two and five generation symmetric physical models. In these experiments, an air flow rate range of 1 to 400 ml/s was investigated with benzene vapor, helium, and sulfur hexafluoride introduced as tracers in separate experiments.

THEORETICAL DEVELOPMENT

Compartmental Representation

For a one-inlet/one-outlet flow system, the extent of tracer mixing is characterized by the variance (σ_t^2) of the concentration impulse response at the flow outlet:

$$\sigma_t^2 \equiv \frac{\int_o^\infty C(t-\bar{t})^2 dt}{\int_o^\infty C dt} \quad (7)$$

where the mean residence time is defined by

$$\bar{t} \equiv \frac{\int_o^\infty Ct dt}{\int_o^\infty C dt} \quad (8)$$

If, in addition, such a system may be subdivided into a series of compartments whose mixing dynamics are not interdependent, then the system variance may be expressed as the sum of the concentration variances contributed by each compartment. For example

$$\sigma_t^2 = \Delta\sigma^2 t_o + \Delta\sigma^2 t_1 + \Delta\sigma^2 t_2 \quad (9)$$

for the series system in Figure 2*a*. Similarly, the mean residence times are additive

$$\bar{t} = \Delta\bar{t}_o + \Delta\bar{t}_1 + \Delta\bar{t}_2 \quad (10)$$

In analyzing a tube network, it is convenient to represent the system as a series-parallel array of compartments; each compartment is intended to correspond to a particular tubular branch in the real system. In this treatment, the regions where branching occurs are considered to be nodes of fluid division. This implies that either the branching regions do not contribute to mixing or that their contribution has artificially been absorbed into the dynamics of adjacent compartments. Thus, the mixing dynamics attributed to each compartment of a network model (Figure 2*b*) must at least account for the tracer dispersion that occurs in the corresponding tubular branch, and it might also account for mixing induced by adjacent branching regions.

A frequent objective in analyzing tube networks is to be able to predict the overall extent of mixing along a particular transport path. In terms of the compartmental model, this implies that the increase in concentration variance caused by each constitutive compartment as well as the proper variance additivity rule must be known. Since σ_t^2 is an Eulerian variable, there at first appears to be a difficulty in arriving at an additivity rule in branched systems where velocity may change across branch nodes. For this purpose, it is easier to discuss the volumetric variance

$$\sigma_v^2 \equiv \dot{V}^2\sigma_t^2 \quad (11)$$

The square root of σ_v^2 represents the fluid volume in which the tracer is effectively distributed. $\dot{V}$ is the volumetric rate of flow. In crossing a branch node, fluid volume is distributed to the downstream compartments in accordance with the relative rate of flow. Thus

$$\sigma^2_{v,i+1} = \left(\frac{\dot{V}_{i+1}}{V_i}\right)^2 \sigma^2_{v,i} \quad (12)$$

is the relationship between the volumetric variance at the outlet of compartment i and that at the inlet of compartment $(i + 1)$. Combination of Equations (11) and (12) yields the equality

$$\sigma^2_{t,i+1} = \sigma^2_{t,i} \quad (13)$$

Thus, for steady state flow through the compartmental network model, branch nodes have no effect upon the variances σ^2_{ti}. This implies that the additivity rule [Equation (9)] is applicable for a string of compartments in a tube network.

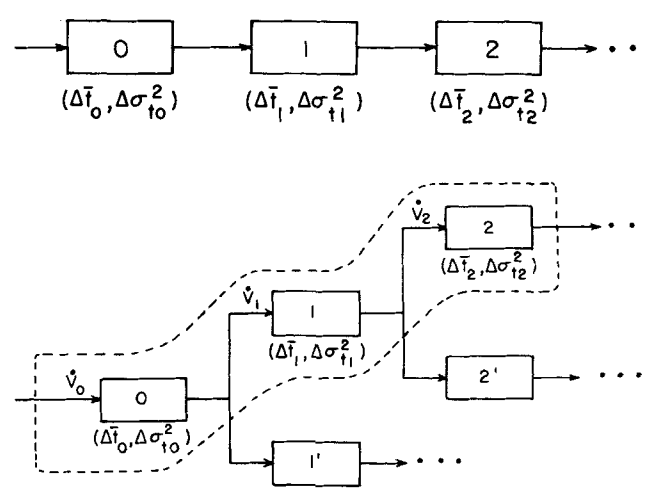

Fig. 2. Compartmental systems models. *a*. Single path system. *b*. Tube network with one possible transport path outlined by the broken envelope. The increase in mean residence time and in tracer dispersion caused by each compartment are represented by $\Delta\bar{t}_i$ and $\Delta\sigma_{ti}^2$, respectively.

TABLE 1. CHARACTERISTICS OF SYMMETRIC PHYSICAL MODELS

Designation	Number of generations	Branch lengths, l_i (cm)	Branch radii, a_i (cm)	Branching angle, θ
Model I	0	18.0	0.85	—
Model II	2	6.0	0.85	70°
Model III	5	Equation (28)	Equation (27)	35°

Compartmental Mixing

In traditional compartmental analysis, an individual compartment is assumed to be perfectly mixed. In our analysis, however, each compartment is considered to be a distributed parameter subsystem in which tracer mixing is described by an appropriate dispersion model. Our rationale for using this approach is that it forms a basis upon which tracer mixing can be predicted once the geometry is specified. The use of perfectly mixed compartments, on the other hand, would only provide a useful model for data correlation.

The dispersion model that we adopt is based upon the solution to Equation (1) for impulse injection at $x = t = 0$ of a quantity M of tracer into a doubly infinite straight tube of cross section S. If we assume axial mixing coefficient is a function of time only, the concentration profile is given by

$$C = \frac{M/S}{2\left(\frac{\pi a^2}{\mathcal{D}}\int_o^\tau D d\tau\right)^{1/2}} \exp\left\{\frac{-\left[x-\left(\frac{ua^2}{\mathcal{D}}\right)\tau\right]^2}{4\left(\frac{a^2}{\mathcal{D}}\right)\int_o^\tau D d\tau}\right\} \tag{14}$$

We now consider the concentration profiles that would be sampled at two points x_1 and x_2 downstream of the injection site $x = 0$. If we assume that dispersion is relatively small (Levenspiel and Smith, 1957), then the change in the concentration variance between the sampling positions can be given by

$$\Delta\sigma_t^2 = \frac{2a^2}{u^2\mathcal{D}}\int_{\tau_1}^{\tau_2} D(\tau)d\tau \tag{15}$$

where the dimensionless time can be approximated in terms of the dimensionless residence time:

$$\tau = \frac{\mathcal{D}}{a^2}\bar{t} = \frac{\mathcal{D}x}{a^2u} \tag{16}$$

We now apply the dispersion model to a given transport path consisting of a series of compartments $i = 0, 1, 2 \ldots, N-1, N$. A tracer impulse is injected into compartment 0 and is sampled at the exit of compartment N. We make the crucial hypothesis that the value of the mixing coefficient in the i^{th} compartment is only a function of the dimensionless residence time (τ_i). This residence time is obtained by summing the individual values for all compartments along the transport path, up to compartment i:

$$\tau_i \equiv \sum_{s=0}^{i}\Delta\tau_s = \sum_{s=0}^{i}\left(\frac{\mathcal{D}l_s}{a_s^2u_s}\right) \tag{17}$$

Here l_s, a_s, and u_s are the length, radius and gas velocity in the tubular branch represented by compartment s. This hypothesis allows the combination of Equations (9) and (15) in order to obtain the overall concentration variance at the exit of compartment N:

$$\sigma_t^2 = \frac{2}{\mathcal{D}}\sum_{i=0}^{N}\left(\frac{a_i}{u_i}\right)^2\int_{\tau_{i-1}}^{\tau_i} D(\tau)d\tau \tag{18}$$

The prediction of the concentration variance using Equations (17) and (18) requires firstly that the branch lengths and radii be known and secondly that the functional form of $D(\tau)$ be stipulated. As a first-order approximation, we adopt the Gill-Sankarasubramanian theory, Equations (2) and (3), for $D(\tau)$. In so doing, we have implicitly assumed that a well-developed laminar velocity profile exists in all compartments and that the shape of the concentration profile is unaltered when the fluid crosses a branch point. Combination of Equations (2), (3), (17), and (18) yields the working equation for the concentration variance:

$$\sigma_t^2 = \frac{8}{\mathcal{D}^2}\sum_{i=0}^{N}[a_i^4]\left\{\frac{\Delta\tau_i}{192}+\left(\frac{a_i}{2l_i}\right)^2\Delta\tau_i^3 + 4\sum_{n=1}^{\infty}\left(\frac{B_n}{\lambda_n^2}\right)[e^{-\lambda_n^2\tau_i}-e^{-\lambda_n^2\tau_{i-1}}]\right\} \tag{19}$$

In this study, we compare the predictions of Equation (19) to data obtained in three symmetric tubular networks of progressively increasing complexity (Table 1 and Figure 1).

Model I: The Straight Tube

This system was selected in order to determine whether or not our experimental techniques yield reliable data for the case where the theory most rigorously applies. For the straight tube, N is equated to zero in Equation (19). Also, since two different tracer gases are studied in the experiments, it is convenient to define a dimensionless variance as

$$\tilde{\sigma}^2 \equiv \frac{\mathcal{D}^2}{8a_o^4}\sigma_t^2 \tag{20}$$

where a_o is a characteristic radius. Combination of Equations (17), (19) and (20) yields

$$\tilde{\sigma}^2 = \frac{\tau}{192}+\left(\frac{a}{2L}\right)^2\tau^3 - 4\sum_{n=1}^{\infty}\left(\frac{B_n}{\lambda_n^2}\right)(1-e^{-\lambda_n^2\tau}) \tag{21}$$

and

$$\tau = \frac{\mathcal{D}\bar{t}}{a^2} = \frac{\mathcal{D}L}{a^2u} \tag{22}$$

where a and L are the radius and length of model I, and a_o has been equated to a.

Model II: The Two-Generation Uniform Diameter Symmetric Tube Network

In symmetric tube networks, the branch generations are labeled sequentially with the mother branch taken as $i = 0$. In the symmetric model II, the branch diameters ($2a$) and branch lengths (l) each had constant values throughout the model. In that case, Equations (19) and (20) become

$$\tilde{\sigma}^2 = \sum_{i=0}^{2}\left\{\frac{\Delta\tau_i}{192}+\left(\frac{a}{2l}\right)^2\Delta\tau_i^3 + 4\sum_{n=0}^{\infty}\left(\frac{B^n}{\lambda_n^2}\right)(e^{-\lambda_n^2\tau_i}-e^{-\lambda_n^2\tau_{i-1}})\right\} \tag{23}$$

where the index i represents the generation number, and a_o has been equated to a.

The summation of the first term on the right-hand side of this equation is equal to $\tau/192$, and summation of the third term is $-4\sum_{n=0}^{\infty}\left(\frac{B_n}{\lambda_n{}^2}\right)(1-e^{-\lambda_n{}^2\tau})$. τ is the total dimensionless residence time defined by

$$\tau=\sum_{i=0}^{2}\frac{\mathcal{D}l}{a^2u_i}=\sum_{i=0}^{2}\frac{\mathcal{D}l}{a^2u_o}2^i \tag{24}$$

where u_o is the velocity through the zeroth generation. In order to compare Equation (23) to the corresponding straight tube formulation [Equation (21)], it is necessary to relate $\sum_{i=0}^{2}(\Delta\tau_i)^3$ to τ. That is

$$\sum_{i=0}^{2}\Delta\tau_i{}^3=\sum_{i=0}^{2}\left(\frac{\mathcal{D}l}{a^2u_o}2^i\right)^3=\frac{\sum_{i=0}^{2}2^{3i}}{\left(\sum_{i=0}^{2}2^i\right)^3}\tau^3 \tag{25}$$

so that Equation (23) becomes

$$\sigma^2=\frac{\tau}{192}+0.2128\left(\frac{a}{2l}\right)^2\tau^3-4\sum_{n=0}^{\infty}\left(\frac{B_n}{\lambda_n{}^2}\right)(1-e^{-\lambda_n{}^2\tau}) \tag{26}$$

which, except for the factor multiplying the axial diffusion term, is the same as the result for the straight tube.

Model III: The Five-Generation Symmetric Tube Network

In the symmetrically branched model studied by Scherer et al. (1975), the branch radii and lengths decrease from generation to generation according to the equations

$$a_i=a_o2^{-i/3} \tag{27}$$

$$l_i=6a_i \tag{28}$$

where the index i corresponds to the generation number. For this particular geometry, the dimensionless residence time in each branch is given by

$$\Delta\tau_i=\left(\frac{l_i}{u_i}\right)\left(\frac{\mathcal{D}}{a_i{}^2}\right)=\frac{6a_i}{(\dot{V}/\pi a_i{}^2 2^i)}\left(\frac{\mathcal{D}}{a_i{}^2}\right)=\frac{6a_o}{u_o}\left(\frac{\mathcal{D}}{a_i{}^2}\right) \tag{29}$$

so that the variance may be found from Equation (19) as

$$\sigma_t{}^2=\sum_{i=0}^{5}\left\{\frac{a_o{}^3 2^{-2i/3}}{4\mathcal{D}u_o}+\frac{12\mathcal{D}a_o 2^{2i/3}}{u_o{}^3}+\left(\frac{32a_o{}^4 2^{-4i/3}}{\mathcal{D}^2}\right)\sum_{n=0}^{\infty}\left(\frac{B_n}{\lambda_n{}^2}\right)(e^{-\lambda_n{}^2\tau_i}-e^{-\lambda_n{}^2\tau_{i-1}})\right\} \tag{30}$$

where τ_i is evaluated by summation of Equation (29) according to the identity in Equation (17).

In presenting their results, Scherer et al. did not report the concentration variance. Rather they defined a mixing coefficient based upon the velocity in the zeroth generation branch. In effect, this is a time averaged mixing coefficient ($\overline{D}$) which can be formulated as

$$\overline{D}=\frac{\sigma_t{}^2u_o{}^2}{2\bar{t}}=\frac{\sigma_t{}^2u_o{}^3}{72a_o} \tag{31}$$

where it has been recognized that the overall dimensional residence time ($\bar{t}$) is given by

$$\bar{t}=\sum_{i=0}^{5}\left(\frac{l_i}{u_i}\right)=\frac{36a_o}{u_o} \tag{32}$$

METHODS AND MATERIALS

In this study, impulse-response data for pure sulfur hexafluoride and pure helium injected into air in separate experiments were obtained in models I and II described in Table 1. Both models were constructed of 1.7 cm I.D. glass tubing. The branch points of model II were constructed by fusing a section of straight tubing to a section of appropriately curved tubing. All tube branches occupied the same plane, and the models were always studied with this plane in a horizontal orientation. Sampling holes, approximately 1.5 mm in diameter and sealed with rubber cement, were located at 3 cm intervals along the upper portion of the tube wall in both models.

Filtered humidified compressed air was metered through a set of high and low sensitivity gas rotometers and was supplied to the model through a 250 cm long calming tube having an inside diameter matched to that of the models. Air flow was always directed from the zeroth-order generation toward the higher-order generations, thereby simulating inspiration of gas into the lungs. A flow rate range of 1 to 400 ml/s was investigated.

The gas tracer was injected through a 1.5 mm diameter capillary tube inserted vertically into the calming tube at its downstream end; the base of this capillary injection tube was plugged while three equally spaced 0.07 mm holes were drilled through the upstream as well as the sidestream tube walls. Compressed tracer gas (1 to 10 lb/in.^{2} abs) was released by momentary (30 to 100 ms) opening of a tuned solenoid valve (series 9 two-way valve, General Valve Corp.) which separated the injection tube from the compressed tracer gas supply. The duration of the electrical impulse opening the valve and the compression pressure were adjusted for each experimental run in order to achieve the smoothest possible tracer concentration records.

Tracer gas concentrations were sampled at the center line of the model tube branches using a double ended 24 gauge capillary needle inserted into the sampling capillary of a respiratory mass spectrometer (RMS3, Gould, Inc.). All data were recorded on a two-channel strip chart recorder (Brush Mark 280, Gould, Inc.) with the spectrometer output occupying one channel and the injection valve impulse recorded on the second channel. The gas sampling-analysis-recording system exhibited a 90% rise time of 100 ms. For any given set of experimental conditions, the tracer concentration was monitored at an upstream sampling site and at a downstream site in separate experiments. In the straight tube model I, the two sampling sites were 18 cm apart. In the branched tube model II, the upstream site was located in the zeroth generation branch, 6 cm upstream of the first branch point, and two (theoretically equivalent) downstream sites were each located 6.0 cm downstream of the entrance of a second generation branch. Both models had an additional 28 cm of straight tubing beyond the downstream sampling points in order to minimize artifacts caused by back diffusion from the atmosphere. In both models I and II,

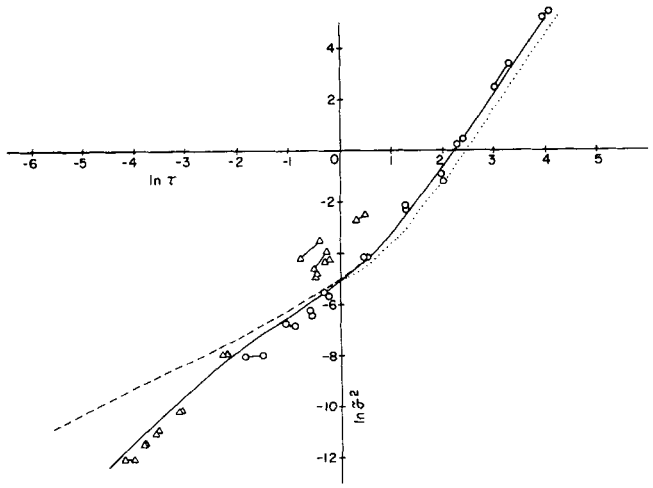

Fig. 3. Comparison of compartmental dispersion theory (———) to the impulse response of helium (○) and sulfur hexafluoride (△) in model II. The lines between points tie the results from the two alternative downstream sampling sites. The theory for model I (· · · ·) is shown as is the theory for model II when unfulfilled dispersion is omitted (- - -).

the distance between the tracer injection tube and the upstream sampling site was 10.7 cm.

At any given flow rate condition, a minimum of sixteen equally spaced data points were read from the recorder outputs, and the values of mean residence time and variance were computed for both the upstream and the downstream sampling sites by applying Simpson's rule to the integrals in Equations (7) and (8). The impulse response at a given flow rate was characterized by the difference between values computed at the upstream and at the downstream sites:

$$\bar{t} \equiv \bar{t}_d - \bar{t}_u \tag{33}$$

$$\sigma_t^2 \equiv \sigma_d^2 - \sigma_u^2 \tag{34}$$

The subscripts u and d indicate upstream and downstream sampling sites, respectively. In the case of data obtained on model II, paired values of $\bar{t}$ and σ_t^2 corresponding to data obtained at the two downstream sampling sites were calculated.

The σ_t^2 were nondimensionalized according to Equation (20). The values for the effective binary diffusivity of helium in air and sulfur hexafluoride in air were computed from the Hirschfelder, Bird, and Spotz equation (Bird et al., 1960) as 0.698 and 0.0923 cm²/s, respectively, at 23°C and 1 atm pressure. The value for the binary diffusivity of benzene vapor in nitrogen, necessary for analyzing the data of Scherer et al. (1975), was computed as 0.0841 cm²/s by the same method.

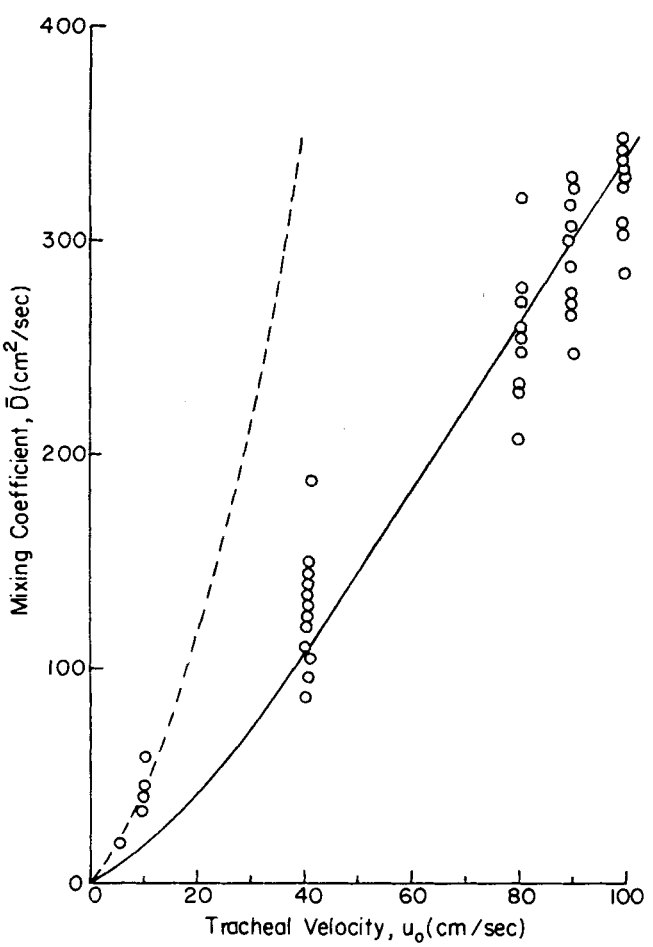

Fig. 4. Comparison of compartmental dispersion theory (———) to the impulse response of benzene vapor (○) in model III. The theory with unfulfilled dispersion omitted (- - -) is also shown. (Data reproduced by permission from Scherer et al., 1975, *J. Appl. Physiol.*, 38, 722).

DISCUSSION AND RESULTS

Theoretical Predictions

The compartmental dispersion theory was applied to three tube networks of progressively increasing complexity. The result for the straight tube model I was obtained from Equations (4), (5), and (21), where the summation was expanded up to and including $n = 4$. The result for the two-generation symmetric model II was similarly obtained from Equations (4), (5), and (26). It is not surprising that these results are quite similar (compare the dotted curve to the solid curve in Figure 3). Firstly, the nondimensionalized Taylor dispersion and the unfulfilled dispersion are independent of branch length and radius when they are evaluated along a transport path of uniform diameter; Secondly, models I and II had the same total transport path lengths so that differences in axial diffusion were minimized. Nevertheless, at values of $\ln\tau > 0.8$, where the extent of mixing by diffusion becomes greater than by Taylor dispersion, the $\tilde{\sigma}^2$ values in model II are 50% larger than those in model I because of the increased cross-sectional area available for diffusion in the branched model.

In the design of their five-generation symmetric tube network (model III), Scherer et al. (1975) provided geometric similarity to Weibel's model 'A' (1963) of the pulmonary tree. Thus, the model was built with a 21% reduction in branch diameter and length across each branch point. Application of the compartmental dispersion theory to predict the mass transport occurring in this model is a significant departure from the basic straight tube theory. Using equations (4), (5), (30), and (31), we have computed the theoretical values of the mean mixing coefficient $\bar{D}$ for benzene in nitrogen when flow is directed from the zeroth toward the higher-order generations (solid curve in Figure 4).

Calculations comparing the magnitude of the various factors contributing to axial mixing were also performed. Firstly, the effect of neglecting the unfulfilled dispersion term was examined. In models I and II, this leads to significant overestimation of axial mixing at the low residence times (compare the broken curve to solid curve in Figures 5 and 3). In model III, this results in an overestimation of mixing for the entire range of tracheal velocities studied by Scherer et al. (compare broken

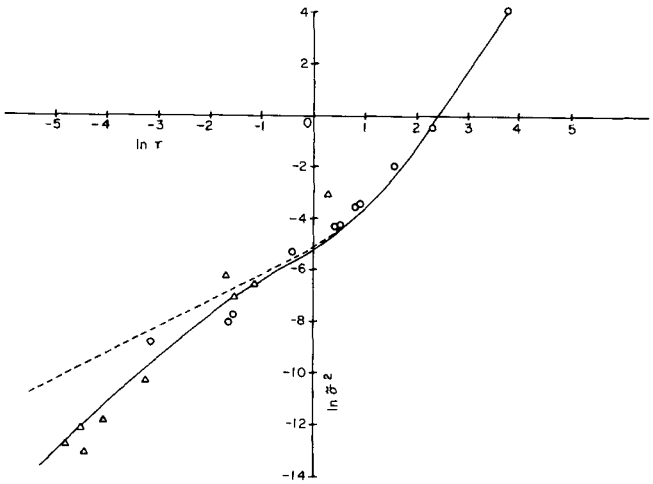

Fig. 5. Comparison of compartmental dispersion theory (———) to the impulse response of helium (○) and sulfur hexafluoride (△) in model I. The theoretical prediction with unfulfilled dispersion omitted is also shown (- - -).

and solid curves in Figure 4). Secondly, the contributions of axial diffusion, Taylor dispersion and unfulfilled dispersion were compared at inspiratory conditions representative of human subjects at rest: $\dot{V} = 500$ ml/s and $\mathcal{D} = 0.25$ cm^2/s for oxygen diffusing in nitrogen. Under these conditions, the dimensionless residence time in model II is 0.066. The corresponding dimensionless variance has a value $1.3(10^{-4})$ of which $3.0(10^{-7})$ is due to axial diffusion, $3.4(10^{-4})$ arises as Taylor dispersion, and a correction of $-2.1(10^{-4})$ must be applied to account for the unfulfilled dispersion. In model III, the stated flow and diffusivity conditions correspond to a value of $\tau = 0.12$. In that case, the dimensionless variance is equal to $1.2(10^{-5})$ and is comprised of contributions of $2.2(10^{-8})$ due to axial diffusion, $7.3(10^{-5})$ due to Taylor dispersion, and a $-6.1(10^{-5})$ correction for unfulfilled dispersion. Thus, in a tube network geometry representative of the first five generations of the human airway system, axial diffusion makes a negligible contribution to overall mixing, and the value of axial dispersion is only 16% of that value predicted by Taylor for a fully developed concentration profile.

Preliminary Experimental Observations

Strict adherence of experimental conditions to the theoretical analysis requires an ideal impulse injection (that is, initially the tracer mass must be uniformly distributed over the tube cross section and injected instantaneously). It also requires that the radially averaged tracer concentration be monitored at the sampling points. Preliminary measurements of the impulse response with sampling at the tube center line, tube wall, and midway between indicated that the tracer volume ($1/\dot{V}\int_0^\infty C dt$) was, to within 10%, uniformly distributed in the radial direction at the upstream sampling position. Moreover, the tracer residence time [Equation (8)] between the upstream and downstream sampling sites was consistent with the mean residence time ($V/\dot{V}$) for values greater than 0.3 s (Figure 6). For values less than 0.3 s, the tracer residence time was always less than the mean residence time. These results may be explained by the fact that the gas sampling velocity was approximately 700 cm/s, while the tube center line velocity, which is twice as large as the mean velocity, ranged from 0.88 to 352 cm/s. Thus, at the highest gas flow rate, the center line velocity approached the value of the sampling velocity. In that case, the sampled gas was representative of the center line tracer concentration which exhibits a residence time that is one half of the mean value. At lower gas flows, however, the relatively high gas sampling velocity resulted in sample withdrawal from a large radial region surrounding the center line so that the monitored tracer concentration was representative of a radially averaged value.

The above observations lead us to conclude that the injected tracer was uniformly distributed by the time it reached the first sampling position and that the center line sampling procedure yielded an adequate representation of radially averaged concentration, at least for residence times greater than 0.3 s corresponding to gas flows less than 140 ml/s. With these conditions met, there is still the problem of correcting for the fact that tracer is not injected instantaneously. In this work, the double sampling procedure [Equations (33) and (34)] suggested by Bishoff (1960) was employed. This technique is strictly valid when the mixing coefficient is constant, which is certainly not the case when unfulfilled dispersion is important. However, calculations employing Equation (21) indicate that the value of $\mathcal{Y}^2$ obtained by double sampling will be in error by no more than 3% for the injector and sampling locations that we have employed.

Comparisons of the Theoretical Predictions to the Data

There is good general agreement between the data and theory in the case of the straight tube model (Figure 5). For the two-generation model II, the data agree well with the theory at extreme values of the dimensionless residence time, but there is data scatter above the curve in the central region. We feel that this scatter is an experimental artifact rather than an effect of tube branching. Note that the data obtained at the two alternate downstream sampling points were quite similar, as expected.

Scherer et al. obtained impulse-response data using the double sampling procedure in model III. Infrared detec-

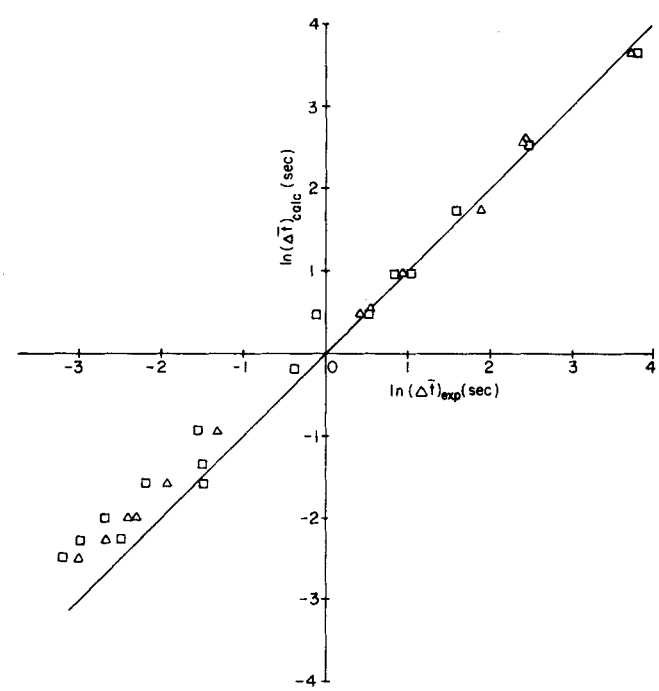

Fig. 6. Consistency of the mean residence time in model I for helium (□) and sulfur hexafluoride (△) tracers. Δt_{calc} is the mean residence time computed on the basis of the volumetric flow rate, while Δt_{exp} is the residence time for tracer computed from Equations (8) and (33).

tion was employed to monitor benzene vapor as a tracer in a pure nitrogen carrier gas. These investigators studied gas velocities in the range of 10 to 100 cm/s, as measured in the zeroth generation. We found excellent agreement between the predictions of the compartmental dispersion theory and their data (Figure 4). As was the case for models I and II, this agreement could not have resulted if unfulfilled dispersion were not taken into account.

The implications of these results are that the extent of longitudinal mixing of a tracer in laminar flow through a tube network may be explained on the basis of the axial diffusion and dispersion that progressively occurs within the tubular brances. The fluid circulation phenomena occurring at branch points (Schroter and Sudlow, 1969) appear to have a negligible quantitative effect in the systems analyzed in this study. Similarly, the deviation of the laminar velocity profile from its ideal parabolic shape seems to have little effect on the mixing.

It must be kept in mind, however, that the experiments in which the compartmental dispersion theory was tested were limited to symmetric tube networks with branch length-to-diameter ratios of 6 and 7. Moreover, flow was always laminar in the direction of increasing branching. With shorter length-to-diameter ratios, the relative effect of branching would become increasingly more important and would eventually have to be accounted for within the compartmental dispersion formulation. Moreover, there is some evidence that branching effects play a more important role when flow is opposite to the direction of increasing branching (Scherer et al., 1975).

ACKNOWLEDGMENT

This work was supported in part by National Science Foundation Grant No. ENG 75-04351 and National Institutes of Health Grant No. HL 17105-01.

NOTATION

a = radius of a tube or tube branch, cm
C = radially averaged tracer concentration ml tracer/ml mixture
$D, \overline{D}, D', \mathcal{D}$ = longitudinal mixing, time average longitudinal mixing, dispersion and molecular diffusion coefficients, respectively, cm^2/s
J_n = Bessel function of order n
l, L = length of a tube branch and total transport path length, respectively, cm
M = volume of pure tracer injected at ambient conditions, cm^3
S = tube cross section, cm^2
$t, \overline{t}, \Delta\overline{t}$ = time, residence time and compartment residence time, respectively, s
u = mean axial velocity, cm/s
V = model volume, cm^3
$\dot{V}$ = volumetric rate of flow, cm^3/s
x = longitudinal position, cm
λ_n = n^{th} root of the Bessel function [see Equation (4)]
$\sigma_t^2, \Delta\sigma_t^2$; = time variance and compartment time variance
$\sigma_v^2; \tilde{\sigma}^2$ (s^2), volumetric variance (cm^6), and dimensionless variance
$\tau, \Delta\tau$ = dimensionless time and compartment dimensionless time, respectively

Subscripts

i, s = integers referring to a particular compartment; the generation number in a symmetric network
u, d = upstream and downstream sampling positions, respectively

LITERATURE CITED

Bartels, J., J. W. Severinghaus, R. E. Forster, W. A. Briscoe, and D. V. Bates. 1954 "The Respiratory Dead Space Measured by Single-Breath Analysis of Oxygen, Carbon Dioxide, Nitrogen, or Helium," *J. Clin. Invest.*, 33, 41-48 (1954).

Bird, R. B., W. E. Stewart, and E. N. Lightfoot, "Transport Phenomena," p. 511, Wiley, New York (1960).

Bishoff, K. B., "Notes on the Diffusion-Type Model for Longitudinal Mixing in Flow," *Chem. Eng. Sci.*, **12**, 69-70 (1960).

Briscoe, W. A., R. E. Forster, and J. H. Comroe, Jr., "Alveolar Ventilation at Very Low Tidal Volumes," *J. Appl. Physiol.*, **7**, 27-30 (1954).

Cumming, G., K. Horsfield, J. G. Jones, and D. C. F. Muir, "The Influence of Gaseous Diffusion on the Alveolar Plateau at Different Lung Volumes," *Resp. Physiol.*, **2**, 386-398 (1967).

Cumming, G., J. G. Jones, and K. Horsfield, "Inhaled Argon Boluses on Man," *J. Appl. Physiol.*, **27**, 447-451 (1969).

Engel, L. A., L. D. H. Wood, G. Utz, J. Joubert, and P. T. Macklem, "Gas Mixing During Inspiration," *ibid.*, **35**, 18-24 (1973).

Gill, W. N., and R. Sankarasubramanian, "Exact Analysis of Unsteady Convective Diffusion," *Proc. Royal Soc.*, **A316**, 341-350 (1970).

Horsfield, K., and G. Cumming, "Morphology of the Bronchial Tree in Man," *J. Appl. Physiol.*, **24**, 373-383 (1968*a*).

———, "Functional Consequences of Airway Morphology," *ibid.*, 384-390 (1968*b*).

Kvale, P. A., J. Davis, and R. L. Schroter, "Effect of Gas Density and Ventilation of Steady State CO Uptake by the Lung," *Resp. Physiol.*, **24**, 385-398 (1975).

Johnson, L. R., and H. D. Van Liew, "Use of Arterial PO_2 to Study Convective and Diffusive Gas Mixing in the Lungs," *J. Appl. Physiol.*, **36**, 91-97 (1974).

Levenspiel, O., and W. K. Smith, "Notes on the Diffusion-type Model for Longitudinal Mixing of Fluids in Flow," *Chem. Eng. Sci.*, **6**, 227-233 (1957).

Power, G. G., "Gaseous Diffusion between Airways and Alveoli in the Human Lung," *J. Appl. Physiol.*, **27**, 701-709 (1969).

Scherer, P. W., L. H. Shendalman, N. M. Greene, and A. Bouhuys, "Measurement of Axial Diffusivities in a Model of the Bronchial Airways," *ibid.*, **38**, 719-723, (1975).

Schroter, R. C., and M. F. Sudlow, "Flow Patterns in Models of the Human Bronchial Airways," *Resp. Physiol.*, **7**, 341-355 (1969).

Taylor, G. I., Dispersion of Soluble Matter in Solvent Flowing Slowly Through a Tube," *Proc. Royal Soc.*, **219A**, 186-203 (1953).

Weibel, E., "Morphometry of the Human Lung," Chapt. 11, Academic Press, New York (1963).

Wilson, T. A., and K. Lin, "Convection and Diffusion in the Airways and the Design of the Bronchial Tree," in "Airway Dynamics," Arend Bohuys, ed., Chapt. 1, Charles C. Thomas, Philadelphia, Pa. (1970).

Yu, C. P., "On Equation of Gas Transport in the Lung," *Resp. Physiol.*, **23**, 257-266 (1975).

Manuscript received April 12, 1976; review completed November 4, 1976. Revised manuscript received December 5, and accepted December 9, 1976.